IFE/KR/E – 2007/001

The paleo heat flow contents in vitrinite reflectance observations

Institute for Energy Technology

	KJELLER	HALDEN
Address	NO-2027 Kjeller, Norway	NO-1751 Halden, Norway
Telephone	+47 63 80 60 00	+47 69 21 22 00
Telefax	+47 63 81 55 53	+47 69 21 22 01

Report number
IFE/KR/E-2007/001

Date
2007-08-27

Report title and subtitle
The paleo heat flow contents in vitrinite reflectance observations

Number of pages
38

Project/Contract no. and name

ISSN
0333-2039

Client/Sponsor Organisation and reference

ISBN
978-82-7017-638-0 (printed)
978-82-7017-639-7 (electronic)

Abstract

The heat flow content in vitrinite reflectance (VR) observations is studied with basis in a simple model of burial at a constant rate. The model is made dimensionless, and it has just one parameter except for the paleo heat flow. The question of existence and uniqueness of a solution is studied, and there exist in general no paleo heat flow that will reproduce a given ("nice") VR-depth curve. But a solution is unique if it exists. A computed VR-depth function is shown to be smooth, even for piecewise constant heat flow histories. The paleo heat flow can be obtained from a VR-depth function after two times with derivations. It is also shown how the present day thermal gradient can be obtained by derivation of a VR-depth representation. The (one-parameter) model allows for approximate expressions for the optimal paleo heat flow as a step function. The results obtained from the one-parameter model are also compared with similar results from a real case study from the North Sea using a state-of-the-art basin simulator.

File (3)

Keywords: vitrinite reflectance

	Name	Date	Signature
Author(s)	Magnus Wangen	2007-08-27	Magnus Wangen
Reviewed by	Ingrid Anne Munz	2007-08-27	Ingrid Anne Munz
Approved by	Harald Johansen	2007-08-27	Harald Johansen

The paleo heat flow contents in vitrinite reflectance observations[1]

Magnus Wangen[2], Torbjørn Throndsen[3] and Gotskalk Halvorsen[2]

[2]Institute for Energy Technology,
P.O.Box 40, N-2027 Kjeller, NORWAY

[3]Querqus,
P.O.Box 2, N-2001, Lillestrøm, NORWAY

ABSTRACT

The heat flow content in vitrinite reflectance (VR) observations is studied with basis in a simple model of burial at a constant rate. The model is made dimensionless, and it has just one parameter except for the paleo heat flow. The question of existence and uniqueness of a solution is studied, and there exist in general no paleo heat flow that will reproduce a given (”nice”) VR-depth curve. But a solution is unique if it exists. A computed VR-depth function is shown to be smooth, even for piecewise constant heat flow histories. The paleo heat flow can be obtained from a VR-depth function after two times with derivations. It is also shown how the present day thermal gradient can be obtained by derivation of a VR-depth representation. The (one-parameter) model allows for approximate expressions for the optimal paleo heat flow as a step function. The results obtained from the one-parameter model are also compared with similar results from a real case study from the North Sea using a state-of-the-art basin simulator.

KEY WORDS: vitrinite reflectance, paleo heat flow, existence of solution, uniqueness of solution

INTRODUCTION

Vitrinite reflectance (VR) is the most widely used thermal maturity indicator in sedimentary basins, and it is also often the only thermal indicator available. The VR values can be grouped into four intervals with respect to hydrocarbon generation: immature, oil generative, gas generative and exhausted, and then provide directly a measure of the maturity of sediment samples. VR is therefore routinely measured in a large number of exploration wells by the oil companies.

The value of VR measurements goes beyond a direct application of the observed values. There are various models that allow VR to be calculated from a given temperature history, (Waples 1980; Larter 1989; Lerche 1990; Sweeney and Burnham 1990; Throndsen 1990; Throndsen, Andersen and Unander 1993). The temperature history can be obtained from thermal modeling of the burial history using the paleo heat flow as input. VR is therefore used to obtain heat flow histories, assuming that the thermal modeling of the burial history is ”sufficiently” accurate. The term ”Thermal Indicator Tomography” was introduced by Lerche, (Lerche 1988; Zhao and Lerche 1993), to describe modeling procedures that invert thermal indicators to reconstruct the thermal history of a well.

Several studies have demonstrated that the paleo temperature contents of the VR measurements along a well is dominated by the maximum sediment temperature, (Gallagher and Sambridge 1992; Vik and Hermanrud 1993; Nielsen 1995; Noeth, Thomsen and Littke 2002; Huvaz, Thomsen and Noeth 2005). This is also an experience basin modelers have made when trying to match VR data by manually tuning a heat flow history.

The sensitivity of VR on the paleo heat flow has been addressed by stochastic (Monte Carlo type of) methods (Nielsen 1996, Gallagher 1998, Ferrero and Gallagher 2002). A large number of heat flow histories are generated, where all histories that reproduce the VR data within certain bounds can be compared. It is then seen that it is impossible to constrain the heat flow history for large parts of the geohistory. Although there exist inversion procedures for obtaining the heat flow history from VR data, (Lerche, Yarzab and Kendall 1984; Lerche 1990; Nielsen 1996; Gallagher 1998), it turns out to be difficult to reconstruct the paleo heat flow without additional geological knowledge, like for instance the timing and the duration of rift episodes.

Very little is known about the heat flow contents in VR observations in terms of analytical results. A simple model, which allows for analytical treatment, is therefore studied. Although the model is simple compared to the complexity

often seen in real burial histories, it turns out that it shows similar VR predictions as with a state-of-the-art basin simulator on a real burial history.

This paper is organized as follows: First is an introduction to VR given. Then follows the simple and dimensionless formulation of the problem of obtaining the paleo heat flow from VR observations. It is shown that an eventual paleo heat flow solution is unique, although a solution cannot be expected to exist. It is then shown that computed VR is a smooth function of depth, and how derivation of a VR-depth-function gives the paleo heat flow. The present day thermal gradient is then obtained from a VR-depth function. The optimal paleo heat flow, as a step function, is found for the simple (dimensionless) model, before a real case is presented, where the results from the simple (dimensionless) model is applied and compared with results from the real model.

TIME-TEMPERATURE-INTEGRAL (TTI) AND VR

There are several approaches to the computation of VR. The simplest models utilize the TTI-concept of Loptin (1971), as for instance done by Waples (1980) and Issler (1984). Models based on Arrhenius kinetics have later been introduced by Burnham and Sweeney (1989), Larter (1989), Sweeney and Burnham (1990). Both types of models are at least semi-empirical where coefficients and Arrhenius data are calibrated with respect to laboratory data and well data. There have also been attempts of a physical based model for VR, see Lerche 1990.

The *TTI* (time-temperature-integral) for a given burial history is the following integral

$$\mathit{TTI} \;=\; \int_{t_1}^{t_2} 2^{(aT(t)+b)}dt \;=\; \int_{t_1}^{t_2} \exp\Big(a_I T(t) + b_I\Big)dt \tag{1}$$

where $T(t)$ is the temperature in ^{o}C as a function of the time t in units Ma. The times t_1 and t_2 are time of the beginning and the end of the burial history, respectively. TTI as an integral is a generalization of the observation made by Lopatin (Lopatin, 1971) that reaction rates double by every step in temperature of $10\ ^o$C. The parameter a is therefore $a = 0.1$, while the parameter $b = -10.5$ is used to make the scaling factor 2^b. (The parameters in the base of the natural logarithm become $a_I = \ln(2)a$ and $b_I = \ln(2)b$.)

VR (%Ro) is correlated to TTI in order to simplify the analytical treatment. There exist different correlations of TTI with (%Ro) and the commonly used functional relationship is

$$\mathit{\%Ro} = \exp\Big(p\ln(\mathit{TTI}) + r\Big) \tag{2}$$

where the parameters p and r have to be fitted to a given data set. Several pairs of p and r parameters have been reported in the literature, see for instance Waples (1980), Issler (1984), and Horváth and others (1988). A comparison of these three parameter sets has been done by Morrow and Issler (1993). Morrow and Issler (1993) have also calibrated expression (2) with the predictions of the popular Easy-%Ro model of Sweeney and Burnham (1990). (All parameters values are listed in table 1.)

A DIMENSIONLESS THERMAL HISTORY

The paleo heat flow content of VR measurements is first studied in a simple model, where burial is at a constant rate, without any compaction of the deposited sediments, and with a single and constant thermal conductivity. These assumptions brings down the number of parameters in the model to just one, when the paleo heat flow is excluded. Such a simple model allows for an analytical formulation of the problem of obtaining the paleo heat flow from VR-measurements. An analytical formulation is interesting in its own right, and it provides more basic insight into the nature of the problem than a purely numerical approach. The results from a simple analytical approach will also to some extent be valid even for real cases with a rather complex geohistory.

A position in the basin is now measured by its height from the basement, which is denoted by the ζ. The ζ-position of a sediment that is deposited becomes a constant, when there is no sediment compaction. The deposition rate, measured as real sediment thickness per time, is ω. The temperature at a ζ-position is then

$$T(\zeta, t) = \frac{Q(t)}{\lambda}\Big(\omega t - \zeta\Big) \tag{3}$$

where $Q(t)$ is the heat flow at time t, and λ is the thermal conductivity. The temperature solution (3) is stationary, and the heat flow is the same at every position along the sedimentary column. Notice that deposition starts at time $t = 0$. A scaled version of the temperature (3) is

$$\frac{T(\zeta, t)}{T_0} = q(\tau)\,(\tau - x) \tag{4}$$

using the reference temperature $T_0 = Q_0 \omega t_0/\lambda$, where Q_0 is todays heat flow and t_0 is the time span of the burial history. The stationary temperature T_0 at the depth $z_0 = \omega t_0$ is the reference temperature. The other dimensionless parameters are dimensionless heat flow $q = Q/Q_0$, dimensionless time $\tau = t/t_0$ and

dimensionless ζ-height $x = \zeta/(\omega t_0)$. The TTI-integral at position x can now be written as $\mathit{TTI}(x) = \mathit{TTI}_0\, I(x)$ where $I(x)$ is the integral

$$I(x) = \int_x^1 e^{k(\tau - x)\, q(\tau)} d\tau \tag{5}$$

and where the parameters are the reference TTI-value $\mathit{TTI}_0 = t_0 e^{b_I}$ and the dimensionless number

$$k = a_I T_0 = \frac{a_I Q_0 z_0}{\lambda} \tag{6}$$

The scaling of time and space makes depth at present time (x) and time of deposition (τ) related by

$$x = \tau \tag{7}$$

VR is given directly by TTI (2), and any VR-observation can therefore be converted to an I-value,

$$\mathit{\%Ro} = c \cdot (t_0\, I)^p \qquad \text{where} \qquad c = e^{p b_I + r} \tag{8}$$

Notice that the time span appears only once, as the coefficient t_0^p, in the TTI-based model for VR. There is just one parameter (k) in the I-integral, apart from the paleo heat flow. Typical values for the k-parameter are in the interval 10 to 20, which corresponds to the temperature interval $T_0 = 100\ ^o$C to $T_0 = 200\ ^o$C.

VR-observations do not provide a continuous curve of depth, but an optimal (continuous) curve $I(x)$ can be fitted to the observations. The challenge is then to obtain the paleo heat flow contents $q(\tau)$ that reproduce the VR data represented by the curve $I(x)$.

EXISTENCE AND UNIQUENESS

The integral (5) is a simple analytical formulation of the problem of obtaining the paleo heat flow from VR-measurements, which allows the questions of uniqueness and existence of a solution to be addressed.

The first fundamental question is whether there exists a function $q(\tau)$ for a "nice" function $I(x)$. The answer is no. Numerical examples show that a function $I(x)$ does not in general have a counterpart $q(\tau)$, not even when $\ln I(x)$ is a simple function like a line or a parabola. The exceptions are the $I(x)$-functions that are made by a given paleo heat flow history $q(\tau)$. In the special case of piecewise constant paleo histories $q(\tau)$ it is always possible to first compute $I(x)$ and then recover the piecewise constant $q(\tau)$ from $I(x)$ by a simple back-substitution scheme as shown in Appendix B. We therefore conclude that it is not possible to

go from an $I(x)$ (or a VR-signal) to an exact paleo heat flow history, even for this basic one-parameter model. The problem of obtaining the paleo heat flow therefore becomes the problem of optimizing the heat flow $q(\tau)$ to obtain a "best" possible match against I-observations.

Related to the existence of a solution is the problem of the uniqueness of a solution. Uniqueness requires that any two heat flow histories $q_a(\tau)$ and $q_b(\tau)$ that yields the same $I(x)$-function have to be equal. The uniqueness of the heat flow solution is shown in Appendix C.

SMOOTHNESS

The integral (5) has the important property of being a "smooth" function, because

$$\frac{dI}{dx} = -1 - \int_x^1 kq(\tau)\, e^{k(\tau - x)\, q(\tau)} d\tau \tag{9}$$

is continuous even for discontinuous heat flow histories. The derivation can also be carried out twice,

$$\frac{d^2I}{dx^2} = kq(x) + \int_x^1 \Big(kq(\tau)\Big)^2 e^{k(\tau - x)\, q(\tau)} d\tau \tag{10}$$

which then yields the heat flow at a given time of burial. Both the left-hand-side and the integral are very large numbers compared to $kq(x)$, except when x is close to 0. It is interesting to notice that the present day heat flow appears for $x = 1$ as

$$q(\tau = 1) = \frac{1}{k} \frac{d^2I}{dx^2}\bigg|_{x=1} \tag{11}$$

where it is used that $x = 1$ corresponds to $\tau = 1$. Differentiation a third time yields

$$\frac{d^3I}{dx^3} = -\int_x^1 \Big(kq(\tau)\Big)^3 e^{k(\tau - x)\, q(\tau)} d\tau - \Big(kq(x)\Big)^2 + k\frac{dq}{dx} \tag{12}$$

which (at least in principle) can be used as an indicator for the sign of $dq/d\tau$ at present time. Then we have that

$$\frac{dq}{dx}(\tau = 1) = kq^2(x = 1) + \frac{1}{k} \frac{d^3I}{dx^3}\bigg|_{x=1} \tag{13}$$

which means that third order behaviour of integral I at the surface tells whether it was a higher or lower heat flow in the past. It is reasonable that these estimates

are for the shallow part of a basin, because the shallow sediments have experienced only the most resent part of the geohistory. These differentiations could have been most useful if the VR-observations at shallow depths were of high quality. However, it is a problem that VR observations and models for VR are of poor quality for short and cold thermal histories. It is therefore difficult to apply these results.

PRESENT DAY HEAT FLOW

It has been recognized for a long time that the present day thermal gradient is contained in the vitrinite signal. The present day thermal gradient is obtained by approximating $d\ln(\%Ro)/dz$ by a straight line. In the simplest cases, where the VR-data plotted as $\ln(\%Ro)$ follow a straight line, we have that

$$\frac{d\ln(\%Ro)}{dz} = -pa_I \frac{T_0}{z_0} \tag{14}$$

where z_0 is the (present day) maximum sediment depth, (see equation (17) in Appendix A for details). This relationship is based on the assumption of a constant paleo heat flow history $q(\tau) = 1$. This simple relationship can be used to see how well burial at a constant rate, with sediments of a constant porosity, fits a given data set.

HEAT FLOW HISTORIES BY A STEP FUNCTION

Using the present day heat flow as a constant heat flow for the entire geohistory is a simple mean to find out if the heat flow has been higher in the past. If the modeled VR is less than what is observed today, then it is clear that the heat flow has been higher in the past. (Assuming that there are no important hiati in the basin). One of the simplest paleo heat flow histories that can be calibrated against observations is a step function, where the heat flow is q_1 for $\tau < \tau_1$, (as shown in figure 1). Calibration of such heat flow histories are first studied using the one-parameter model for VR. We then have to calibrate both the step size q_1 and the time τ_1 of the step. A family of step functions that gives a reasonable match against the observation is found by requiring that the VR-results from the step function fit the data at the base of the well. Even if the base of the well is a limited part of the VR-observations, it turns out heat flow histories that match the lower part of the VR data will also match the upper part of the VR data fairly well. Let the VR-data at the base of the well be a factor f_R higher than modeled VR using the present day heat flow for the entire basin history. The calibration of

the paleo heat flow as a step function in the simple one-parameter model (5) gives that any step function with

$$q_1 \approx \frac{k + (\ln f_R)/p}{k\tau_1} \tag{15}$$

gives an approximate match against the observations at the base of the well, (see equation (20) in Appendix A for details). The approximation is quite accurate for $\tau_1 > 1/2$.

Different step functions and the related VR is shown in figures 2 and 3. Figure 2 shows the computed VR for 4 step functions, when the calculated VR is a factor 1.1 higher at the base than the reference VR. (The reference VR is obtained using the present day heat flow for the entire geohistory.) Figure 2a and figure 2b show that the VR for the different step functions does not differ very much. The step functions are shown in figure 2c, which shows both the step size and the approximated step size (15). It is not much room for calibration in this case, because the family of step functions gives close VR-curves.

Figure 3 shows the situation when the calculated VR is a factor 1.5 higher at the base than the reference VR. The family of step functions generate VR-functions that are separated roughly as much as 0.5 (%). The step functions with the approximate step size is shown in figure 2c. It is noticed that $\ln(\%Ro)$ is still quite linear.

It is seen from figure 2 and 3 that it is difficult to modify the modeled VR-curve unless the heat flow has been substantial higher in the past. Furthermore, the step-function approach is useful because it bounds the space of possible modeled VR, by the respective heat flow histories.

The opposite situation is when present day heat flow leads to modeled VR that is too high compared to the VR-measurements. This situation, where the heat flow has been less in the past, can also be calibrated with step functions. Figure 4 shows that only a short pulse with the present days heat flow is necessary to achieve the observed VR at the base of the basin. The VR at the base of the basin in figure 4 is a factor 0.9 of what is observed. Figure 4 shows that a constant heat flow $q = 0.96$ or a "short" pulse with length $\Delta\tau = 0.08$ of the present day heat flow $q = 1$ both give nearly the same modeled VR. It is therefore difficult to find any paleo heat flow content in the VR observations for cases where the present day heat flow gives higher VR-values than the observations. (These two situations corresponds to a weight $w = 0$ and $w = w_{\max}$, respectively, in expression (22) for q and expression (24) for τ_1 as shown in the Appendix A.)

A CASE EXAMPLE

VR measurements along a well in the North Sea is used as an example to study how heat flow histories represented by simple step-functions can be calibrated. It is a deep well which has undergone more or less continuous burial, as shown in figure 5. There are good quality VR data throughout the well section, including some excellent data from coaly material at about 4000 m. Log-values of the VR-data are plotted in figure 6a as a function of depth. They are seen to be well represented by a straight line. The line shown is the optimal line from least square fitting of the points. Equation (14) shows that the simple model of burial at a constant rate with a constant paleo heat flow, with sediments of a constant thermal conductivity, gives a straight line when VR is plotted as log-values of depth. The optimal (least square root) line through the data in figure 6a has the steepness 0.00052, and then the parameter values $p = 0.211$ and $a_I = 0.06931$ 1/^{o}C give that $T_0/z_0 \approx 34$ ^{o}C/km. This is in good agreement with the present day temperature $T_0 = 184$ ^{o}C at depth $z_0 = 5.3$ km below the seafloor as shown in figure 6b. The parameter value p that gives a good fit ($p = 0.211$) is between the p-parameter values suggested Waples ($p = 0.2413$) (Waples, 1980) and Issler ($p = 0.1617$) (Issler, 1984).

VR was also modeled using the basin simulator BAS (developed at Institute for Energy Technology, Norway), which solves for transient paleo temperature and VR during burial. The sediment compaction is modeled with a porosity as an exponential function of depth, $\phi = \phi_0 \exp(-z/z_c)$, where ϕ_0 is the surface porosity, z is the depth from the seafloor, and z_c is a depth that characterizes the compaction. The thermal conductivity of the sediments is the geometric mean $\lambda = \lambda_f^{\phi} \lambda_s^{(1-\phi)}$ of the fluid thermal conductivity λ_f and the sediment matrix thermal conductivity λ_s. The parameter values for the porosity and the thermal properties of the sediments are typical for silty shale, (see table 1).

It is assumed that the burial history and the thermal properties of the sediments are correct. The heat flow history is then the only unknown. The starting point for calibrating the paleo heat flow is an estimate for the present day heat flow. The present day heat flow is taken to be 0.05 Wm^{-2}, which is a typical value for heat flow in the area. It is seen that the present day heat flow is not sufficient to achieve the maturity of the data. Heat flow histories represented by a step function were calibrated against the data to see if the heat flow could have been increasing backwards in time. The time of the step is in intervals of 30 Ma from present time and backwards in time until -60 Ma.

The optimal VR-values and the VR-observations are shown in figure 7a. Two of the optimal curves cover the VR-data quite well, which is also seen from the plot of the object function at each time of the steps in figure 7b. The object function is the root-mean-square of the difference between the observations and the

calculated values. (The match is against the entire data set, not just VR at the base of the well.) A slight increase in the deviation from the data at the optimal heat flow is seen with increasing time of the step function. The object function is also becoming wider around the optimal point as the time of step becomes further away. The results therefore support a constant heat flow of 0.066 Wm^{-2} until present, (which is represented by the step function with the step at present time). The object function can be used as a direct measure of the sensitivity of VR for the paleo heat flow. The different optimal heat flow histories are plotted in figure 7c. The size of the step in the optimal heat flow histories are seen to increase in a similar fashion to the (dimensionless) step-height given by equation (15). A comparison with equation (15) is shown in figure 7d, where constant burial is assumed for the last 150 Ma. There is a correspondence between the results, although the simple model is based on a constant deposition rate and a match against one VR value at the base of the well. The k-parameter is 11.0 and the f_R-factor 1.6 in the simple model. (The k is based on the temperature at depth of the deepest VR measurement, which is $T_0 = 160$ ^{o}C at the depth $z_0 = 4500$ m. The f_R factor is the deepest VR measurement divided by the modeled VR at the same depth using the constant 0.05 Wm^{-2} for the heat flow history.) The simple model can also be used for cases where VR is simulated with the Easy-Ro model, by simply calibrating the TTI-based method against the Easy-Ro results.

CONCLUSION

The paleo heat flow content in VR measurements has been studied with basis of a simple model of burial at a constant rate, using Lopatin's TTI-model for VR. The model is simple and therefore allows for a dimensionless formulation with just one parameter except for the heat flow history. It is shown how a simple back-substitution procedure could produce a piecewise constant the paleo heat flow with an arbitrary resolution. Tests using the procedure show that a solution does not in general exist. Furthermore, it is shown that if a solution exists then it is unique. The computed VR of depth is a smooth function, and the second derivative can (in principle) be used to obtain the paleo heat flow. The derivative of the VR-depth-function at the surface gives the surface heat flow. It is then shown how the present day thermal gradient can be obtained from VR-data. The simple (one-parameter) model of VR allows for simple approximate expressions for the optimal paleo heat flow represented by step functions. Finally, the results from the simple (one-parameter) model are compared with similar results obtained for a real case from the North Sea of high quality VR measurements, and a corresponds is seen between the results.

ACKNOWLEDGEMENT

The authors are grateful for the remarks of an anonymous referee.

REFERENCES

Burnham, A.K. and Sweeney, J.J., 1989, A chemical kinetic model of vitrinite maturation and reflectance: Geochimica et Cosmochimica Acta, v. 53, no. 10, p. 2649-2657.

Ferrero, C. and Gallagher, K., 2002, Stochastic thermal history modelling. 1. Constraining heat flow histories and their uncertainty: Marine and Petroleum Geology, v. 19, p. 633-648.

Gallagher, K., 1998, Inverse thermal history modelling as a hydrocarbon exploration tool: Inverse Problems, v. 14, p. 479-497.

Gallagher, K. and Sambridge, M., 1992, The resolution of past heat flow in sedimentary basis from nonlinear inversion of geochemical data: the smoothest model approach with synthetic examples: Geophysical Journal International, v. 109, p. 78-95.

Horváth, F., Dövényi, A., Szalay, and Royden, L.H., 1988, Subsidence, thermal and maturation history of the Great Hugarian Plain, Pannonian basin - a study in basin evolution, in, Royden, L.H. and Horváth, F., ed., AAPG Memoir, v. 54, p. 986-996.

Huvaz, O., Thomsen, R.O., and Noeth S., 2005, A method for analysing geothermal gradient histories using the statistical assessment of uncertainties in maturity models: Journal of Petroleum Geology, v. 28, (2), p. 107-118.

Issler, D.R., 1984, Calculation of organic maturation levels for offshore eastern Canada - implications for general application of Lopatin's method: Canadian Journal of Earth Sciences, v. 21, p. 477-488.

Larter, S., 1989, Chemical models of vitrinite reflectance evolution: Geologische Rundschau, v. 78 (1), p. 349-359.

Lerche, I., 1988, Inversion of multiple thermal indicators: quantitative methods of determining paleo-heat flux and geological parameters. I. Theoretical development for paleo-heat flux: Mathematical Geology, v. 20, no. 1, p. 1-36.

Lerche, I., Yarzab, R.F. and Kendall, C.G., 1984, The determination of paleo-heat flux from vitrinite reflectance data: AAPG Bulletin, v. 68, p. 1704-1717.

Lerche, I., 1990, Basin analysis: Quantitative methods 1: Academic Press, London, 562 p.

Lopatin, N.V., 1971, Temperature and geolocial time as a factor in coalification:

Izv. Akad. Nauk. SSSR, Ser. Geol., v. 3, p. 95-106.

Morrow, D.W. and Issler, D.R., 1993, Calculation of vitrinite reflectance from thermal histories: A comparison of some methods: AAPG Bulletin, 77, no. 4, 610-624.

Nielsen, S.B., 1995, An upper limit to paleo heat flow: theory and examples from the Danish Central Graben,: Tectonophysics, v. 244, p. 137-152.

Nielsen, S.B., 1996, Sensitivity analysis in thermal and maturity modelling: Marine and Petroleum Geology, v. 13, no. 4, p. 415-425.

Noeth, S., Thomsen, O. and Littke, R., 2002, A method for assessing statistical significance and uncertainties for calibration of 1-D thermal maturation models: AAPG Bulletin, v. 86, no. 3, p. 417-431.

Sweeney, J.J. and Burnham, A.K., 1990, Evaluation of a simple model of vitrinite reflectance based on chemical kinetics: Am. Assoc. Pet. Geol., Bull., v. 74, p. 1559-1570.

Throndsen, T., 1990, Scatter in vitrinite reflectance data from coal samples in North Sea wells: Norsk Geologisk Tidsskrift, v. 70, p. 223-228.

Throndsen, T., Andersen, B. and Unander, Å., 1993, Comparison of different models for vitrinite reflectance evolution using laboratory calibration and modelling of well data, in, Doré, A.G, ed., Basin modelling: Advances and Applications, NPF Special publication 3, Elsevier, Amsterdam, p. 127-133.

Vik, E. and Hermanrud, C., 1993, Thermal effects of rapid subsidence in the Haltenbanken area, in, Doré, A.G., ed., Basin modelling: Advances and Applications, NPF Special publication 3, Elsevier, Amsterdam, p. 107-117.

Waples, D.W., 1980, Time and temperature in petroleum formation: application of Lopatin's method to petroleum exploration: Am. Assoc. Pet. Geol., Bull., 64, p. 916-926.

Zhao, K. and Lerche I., 1993, Thermal maturation and burial history of the Multiwell Experiment Site, Piceance Basin, Colorado: application of thermal indicator tomography, in, Doré, A.G., Basin modelling: Advances and Applications, NPF Special publication 3, Elsevier, Amsterdam, p. 135-145.

APPENDIX A (OPTIMAL STEP HEAT FLOW HISTORY)

Integral (5) becomes

$$I_0(x) = \frac{1}{k}\Big(e^{k(1-x)} - 1\Big) \approx \frac{1}{k} e^{k(1-x)} \tag{16}$$

for a constant heat paleo heat flow $q(\tau) = 1$. VR in this case is then

$$\begin{aligned} \ln(\%Ro) &= p\ln I + p\ln t_0 + pb_I + r \\ &= pk(1-x) + p\ln(t_0/k) + pb_I + r \end{aligned} \tag{17}$$

which shows that $\ln(\%Ro)$ becomes a line except for x close to 1. The integral (5), in case of a step-function, is

$$I_s(x) = \int_x^{\tau_1} e^{kq_1(\tau - x)} d\tau + \int_{\tau_1}^{1} e^{k(\tau - x)} d\tau \tag{18}$$

for $x < \tau_1$. When the integral I_s is a factor f_I larger than I_0 at the base of the basin (at $x = 0$) we have that

$$\frac{1}{kq_1} e^{kq_1\tau_1} + \frac{1}{k}\Big(e^k - e^{k\tau_1}\Big) \approx f_I \frac{1}{k} e^k \tag{19}$$

which can be approximated as

$$\frac{1}{q_1} e^{kq_1\tau_1} \approx f_I e^k \tag{20}$$

because the factor f_I may typically be of order 10. The factor f_I follows from the corresponding VR-factor f_R at the base of the basin, where f_R is the ratio of VR from $I_s(0)$ over VR from $I_0(0)$. The factor f_I is therefore related to f_R as $f_I = (f_R)^{1/p}$. Equation (15) follows by using ln on both sides of equation (20).

The situation when the integral $I_s(0)$ is a factor f_I less than $I_0(0)$ can be treated by letting the two parts of the geohistory be counting for $(1 - w)$ and w of the right-hand-side $f_I\, I_0(0)$, where w is a unit weight. When

$$\frac{1}{k}\Big(e^k - e^{k\tau_1}\Big) = w f_I \frac{1}{k} e^k \tag{21}$$

we get that

$$\tau_1 = 1 + \frac{1}{k}\ln(1 - w f_I) \tag{22}$$

The first part of the geohistory is then $(1-w)f_I\, I_0(x)$, which gives that

$$q_1\tau_1 \approx 1 + \frac{1}{k}\ln((1-w)f_I) \tag{23}$$

or

$$q_1 \approx \frac{k + \ln((1-w)f_I)}{k + \ln(1-wf_I)} \tag{24}$$

Both τ_1 and q_1 is then parameterized by the unit weight w. The weight cannot be any number in the range 0 to 1. The minimum value $w = 0$ gives $\tau_1 = 1$ and $q_1 = 1 + (1/k)\ln(f_I)$, and the upper limit for w is $w_{\max} = 1 - (1/f_I)e^{-k}$. For $w = w_{\max}$ we get that $q_1 = 0$ and that $\tau_1 = 1 + (1/k)\ln(1 + e^{-k} - f_I)$. Using $w = w_{\max}$ it is only necessary to include the last part of the geohistory ($\tau > \tau_1$) to obtain the wanted VR-value at the position $x = 0$.

APPENDIX B (BACK-SUBSTITUTION)

It is now assumed that there exists a piecewise constant heat flow history that gives the function $I(x)$. The burial history is discretized as shown in figure 8, where time (τ) and (x) are discretized with the same step size. The time of deposition τ_i is the same as the position x_i, and the heat flow is q_i in the interval τ_{i-1} to τ_i. There are n steps of size $\Delta x = \Delta\tau = 1/n$, (see figure 8). The given VR at each x_i position is transformed to an observed I-value $I_{obs,i}$.

The most recent piece in the heat flow history (q_n) is found from I-observation $I_{obs,(n-1)}$, by solving for the heat flow from the equation

$$\int_{x_{n-1}}^{1} e^{k(\tau - x_{(n-1)})q_n}\, d\tau = I_{obs,(n-1)} \tag{25}$$

or

$$\frac{1}{kq_n}\Big(e^{k\Delta\tau q_n} - 1\Big) = I_{obs,(n-1)} \tag{26}$$

This is the same as solving $(e^u - 1)/u = I_{obs,(n-1)}/\Delta\tau$ for u, which has a solution if $I_{obs,(n-1)}/\Delta\tau > 1$.

The scheme above can be carried out iteratively until q_1 is found by using the known heat flow steps q_n, q_{n-1}, ..., q_{i+1} to find heat flow step q_i. The I-observation at the depth x_{i-1} is

$$\begin{aligned} I_{obs,(i-1)} &= \int_{x_{i-1}}^{1} e^{k(\tau - x_{(i-1)})q(\tau)}\, d\tau && (27)\\ &= \frac{1}{kq_i}\Big(e^{k\Delta\tau q_i} - 1\Big) && (28)\\ &+ \sum_{j=i+1}^{n} \int_{x_{j-1}}^{x_j} e^{k(\tau - x_{(i-1)})q_j}\, d\tau && (29) \end{aligned}$$

Notice that heat flow steps q_j with $j = i + 1$ to n are known in the sum (29). The difference between the sum (29) and the I-value $I_{obs,(i-1)}$ is denoted ΔI, which leads to the equation

$$\frac{1}{kq_i}\left(e^{k\Delta\tau q_i} - 1\right) = \Delta I \tag{30}$$

for the next heat flow step q_i.

APPENDIX C (UNIQUENESS)

Uniqueness of the heat flow history is proved by assuming that there exist two different heat flow functions $q_a(\tau)$ and $q_b(\tau)$, which give the same integral $I(x)$, and where both functions are assumed to be smooth. The two functions $q_a(\tau)$ and $q_b(\tau)$ are compared on the interval $[0, 1]$, and because they are unequal and smooth, there must exist open subintervals $U_i =< \alpha_i, \beta_i >$, where $q_a > q_b$ (or $q_a < q_b$) on the entire interval. The q-functions are equal on the closed interval $V_i = [\beta_i, \alpha_{i+1}]$ between U_i and U_{i+1}, where the closed intervals V_i may be just one point, $\beta_i = \alpha_{i+1}$. (Such single points may be where the difference $q_a(\tau) - q_b(\tau)$ changes sign.) It is assumed that there is a finite number n of points α_i and β_i, where $\beta_0 = 0$ and $\alpha_{n+1} = 1$.

The proof begins with the last closed interval $V_{n+1} = [\beta_n, \alpha_{n+1}]$, (which may be just the point $\beta_n = \alpha_{n+1} = 1$). For this interval we have (by definition) that $q_a = q_b$. Let x be any point in the next interval U_n (towards the left), and we have that

$$\int_x^1 f(x, \tau)\, d\tau = 0 \tag{31}$$

for $x \in [0, 1]$, where

$$f(x, \tau) = e^{k(\tau - x)q_a(\tau)} - e^{k(\tau - x)q_b(\tau)} \tag{32}$$

The integral (31) becomes

$$\int_x^{\beta_n} f(x, \tau)\, d\tau = 0 \tag{33}$$

because $q_a = q_b$ for $\tau \in [\beta_n, 1]$. We have that $q_a > q_b$ (or $q_a < q_b$) for all $\tau \in U_n$, and therefore $\int_x^{\beta_n} f(x, \tau)\, d\tau \neq 0$, which is a contradiction. The functions q_a and q_b are therefore equal on the entire open interval U_n.

The argument is repeated in the same way for the next closed and open intervals to the left (V_i and U_i) until last interval V_0, and $q_a(\tau) = q_b(\tau)$ for all $\tau \in [0, 1]$. Two heat flow histories $q_a(\tau)$ and $q_b(\tau)$, which give the same VR, must therefore be equal.

TABLES, FIGURES AND CAPTIONS

Symbol	Value	Units	Comment
a	0.1	1/^{o}C	see equation (1)
b	-10.5	-	see equation (1)
a_I	0.06931	1/^{o}C	see equation (1)
b_I	-7.27805	-	see equation (1)
p	0.2105	-	see equation (2)
r	-1.26	-	see equation (2)
ϱ_s	2650	kg/m^3	sediment matrix density
c_s	1000	J/kgK	sediment matrix heat capacity
λ_s	2.5	W/Km	sediment matrix thermal conductivity
λ_f	0.63	W/Km	fluid thermal conductivity matrix
ϕ_0	0.45	-	surface porosity
z_c	2500	m	compaction depth

Table 1.

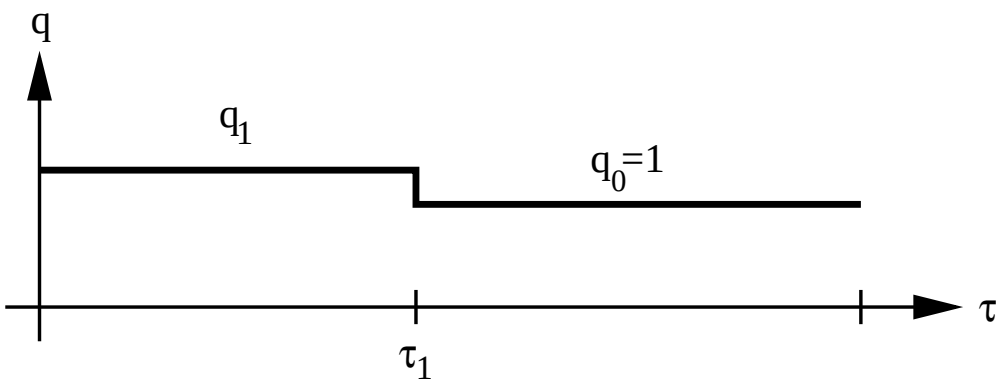

fig1.eps

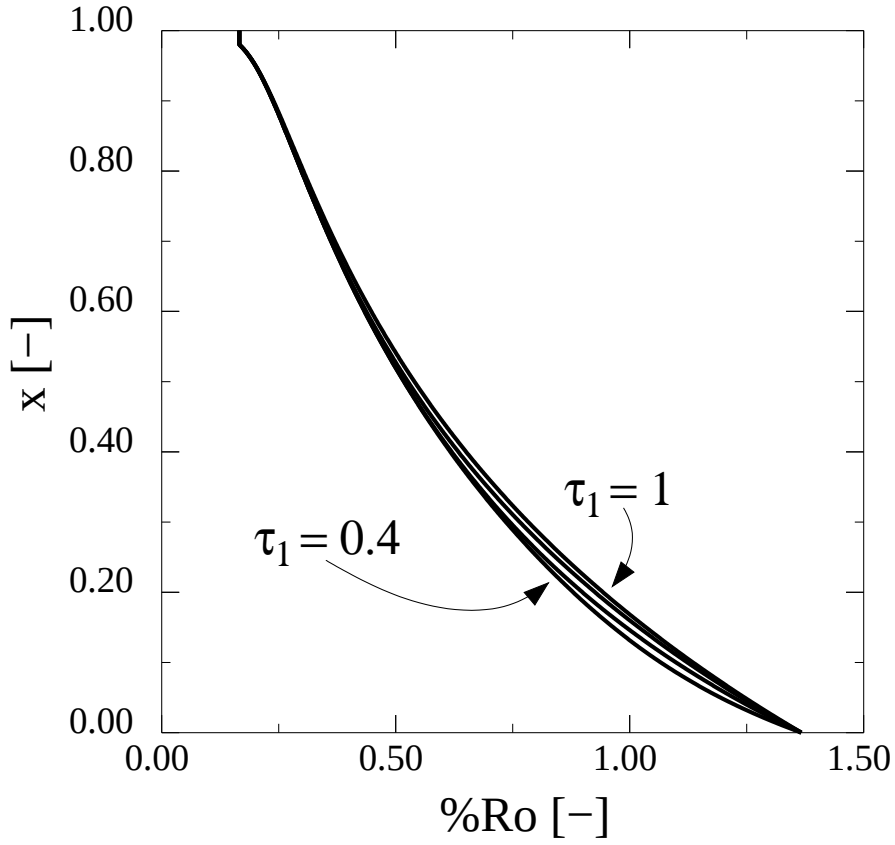

fig2a.eps

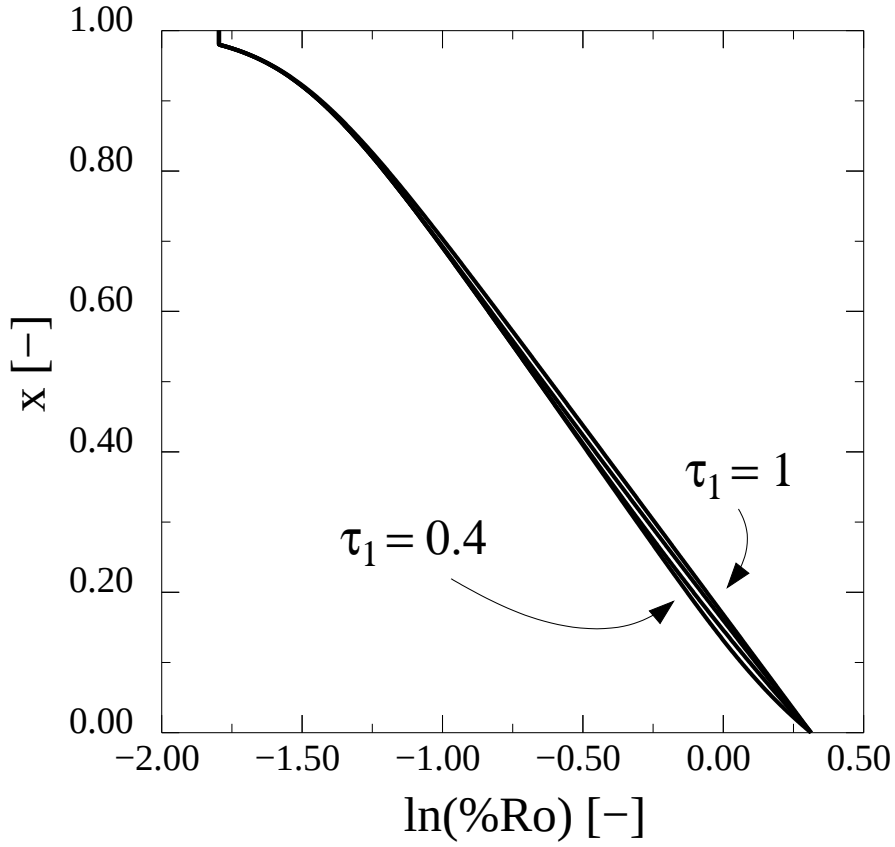

fig2b.eps

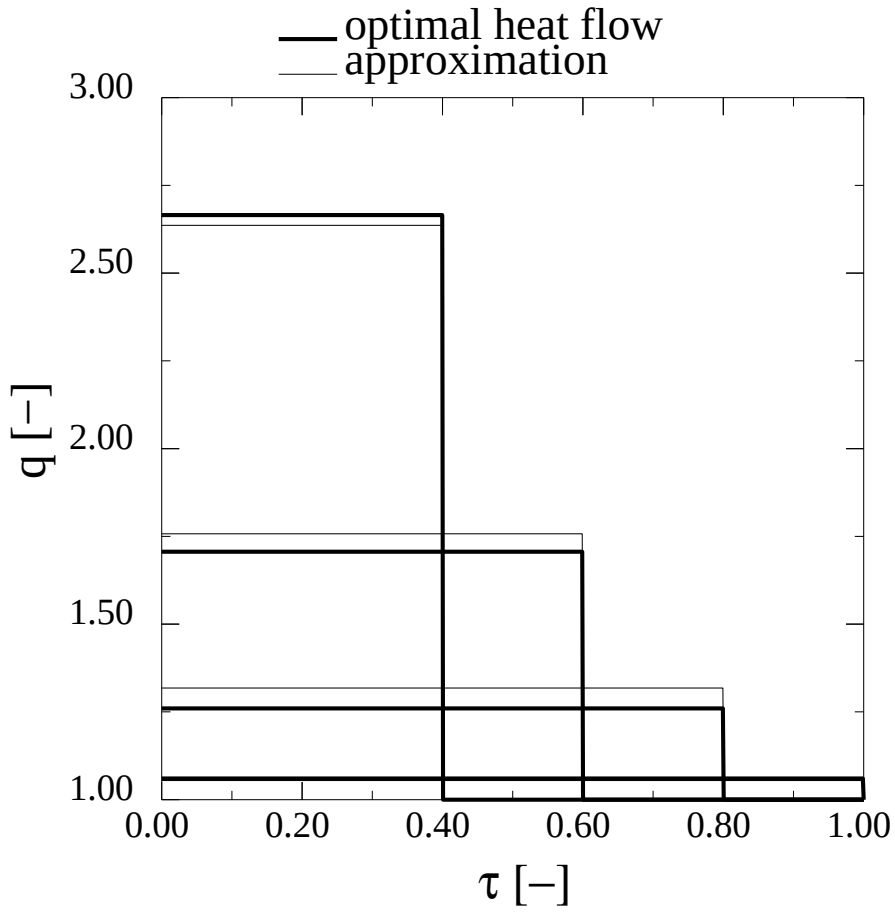
optimal heat flow
approximation
3.00
2.50
2.00
1.50
1.00
q [–]
0.00
0.20
0.40
0.60
0.80
1.00
τ [–]

fig2c.eps

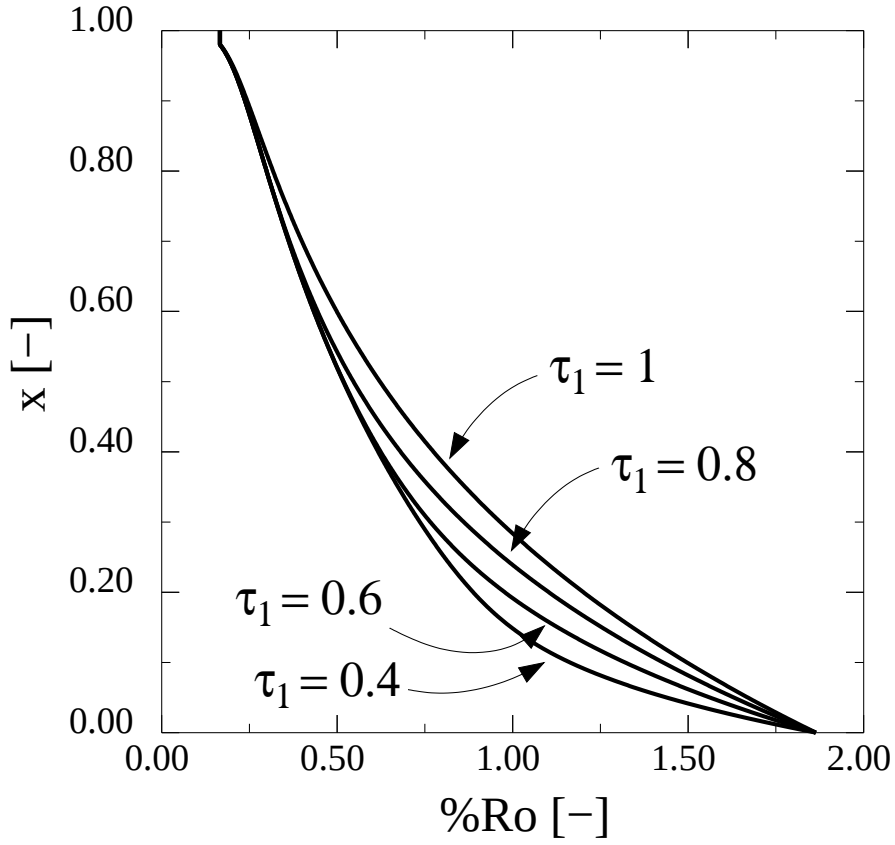
1.00
0.80
0.60
0.40
0.20
0.00
x [−]
0.00
0.50
1.00
1.50
2.00
%Ro [−]
τ1 = 1
τ1 = 0.8
τ1 = 0.6
τ1 = 0.4

fig3a.eps

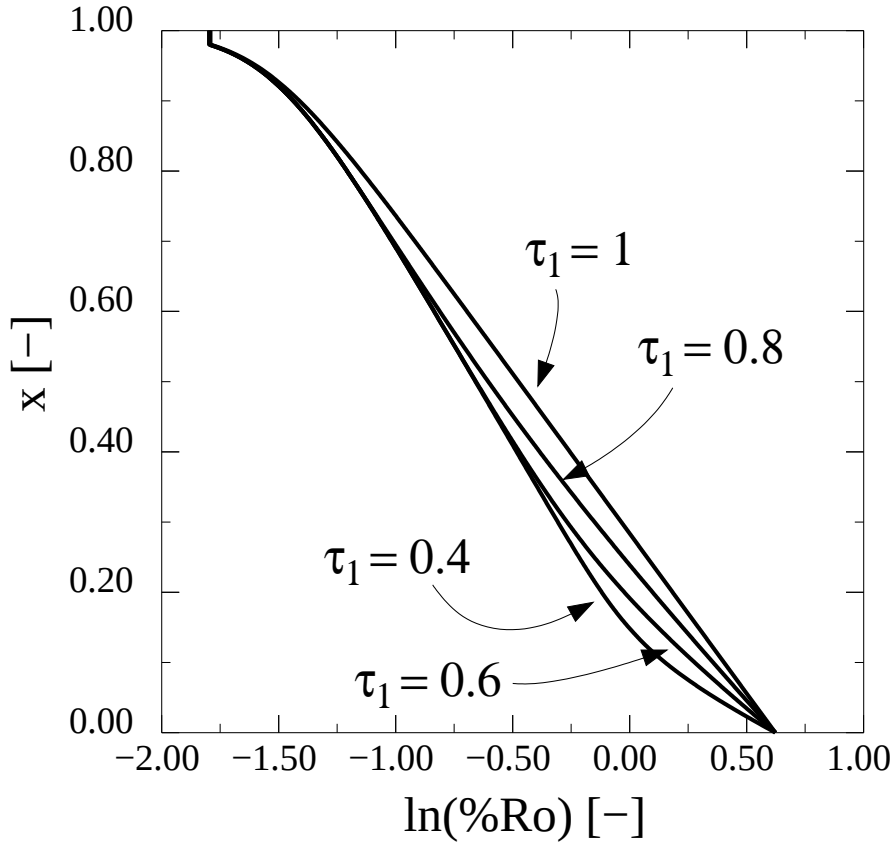
1.00
0.80
0.60
0.40
0.20
0.00
x [−]
−2.00
−1.50
−1.00
−0.50
0.00
0.50
1.00
ln(%Ro) [−]
τ1 = 1
τ1 = 0.8
τ1 = 0.4
τ1 = 0.6

fig3b.eps

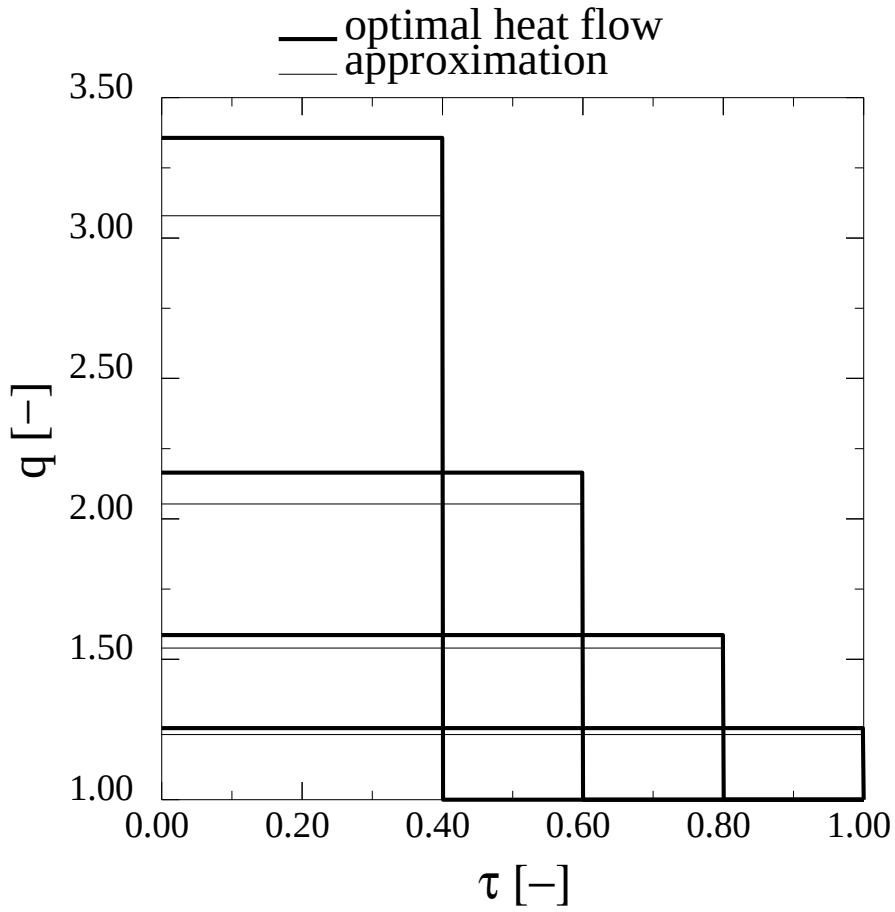
optimal heat flow
approximation
3.50
3.00
2.50
2.00
1.50
1.00
q [–]
0.00
0.20
0.40
0.60
0.80
1.00
τ [–]

fig3c.eps

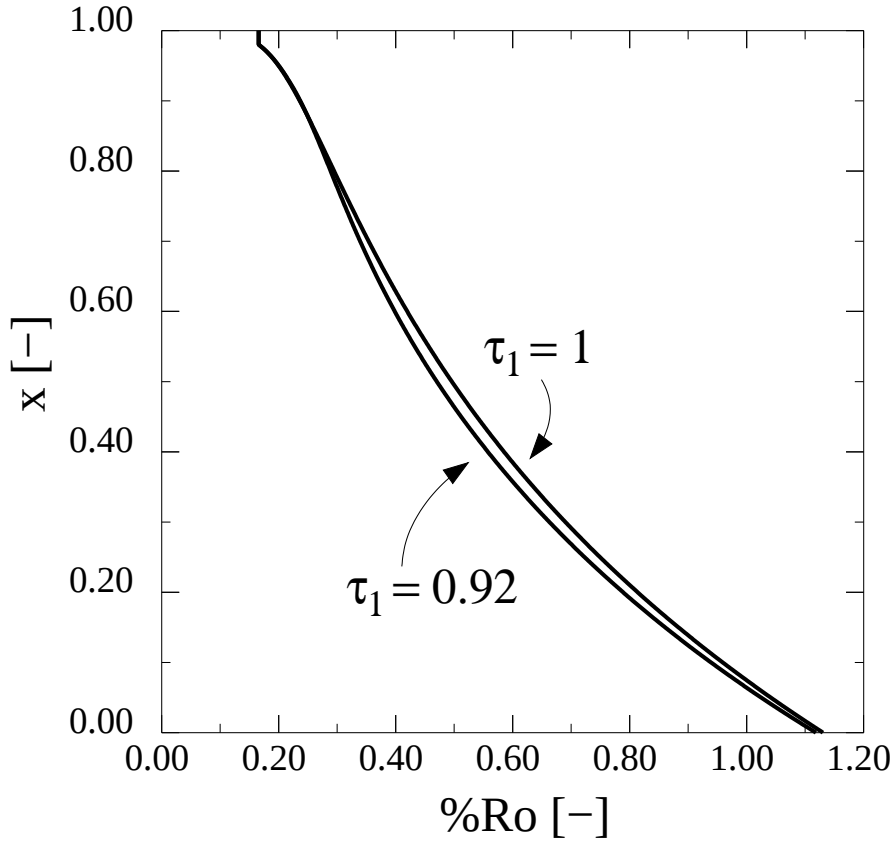
1.00
0.80
0.60
0.40
0.20
0.00
x [−]
0.00
0.20
0.40
0.60
0.80
1.00
1.20
%Ro [−]
τ1 = 1
τ1 = 0.92

fig4a.eps

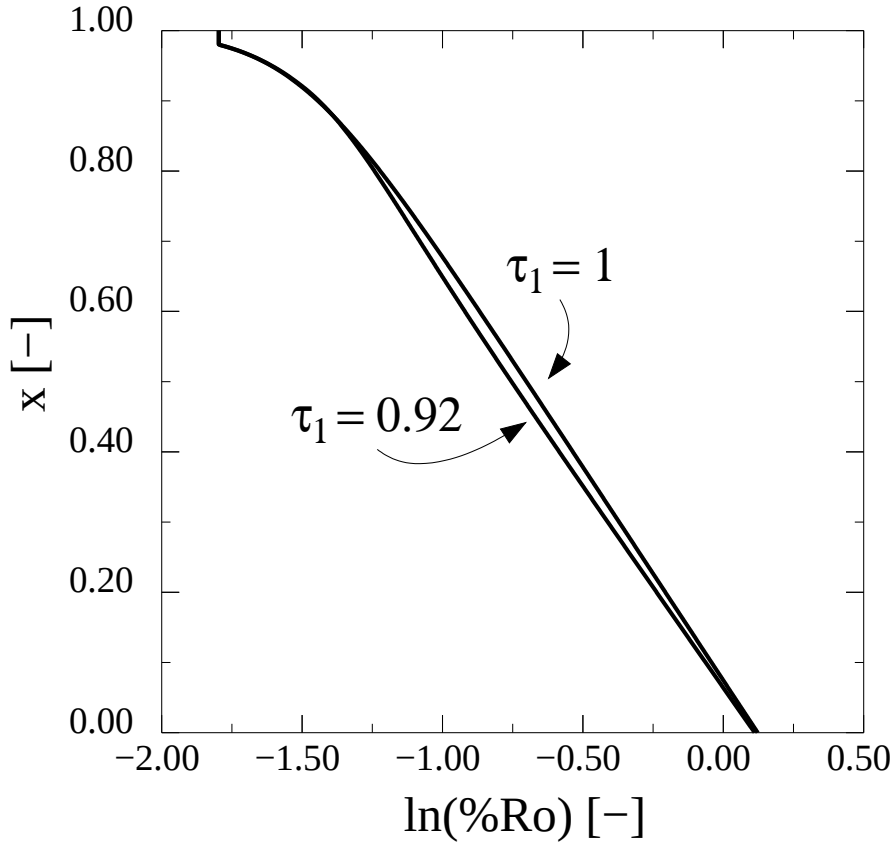

fig4b.eps

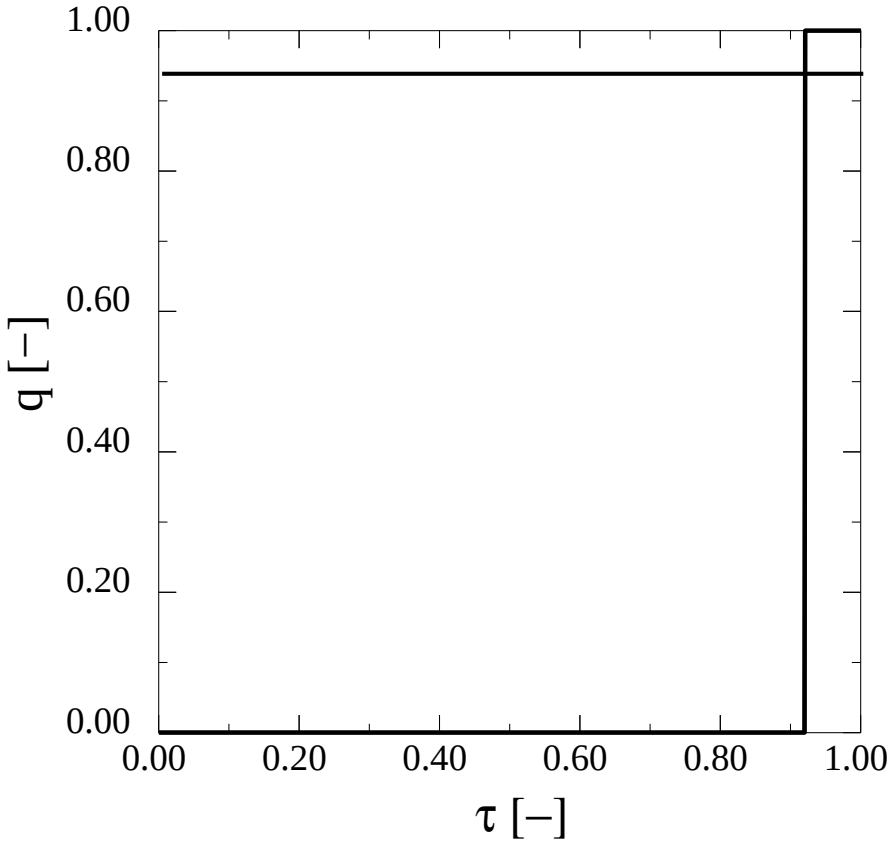

fig4c.eps

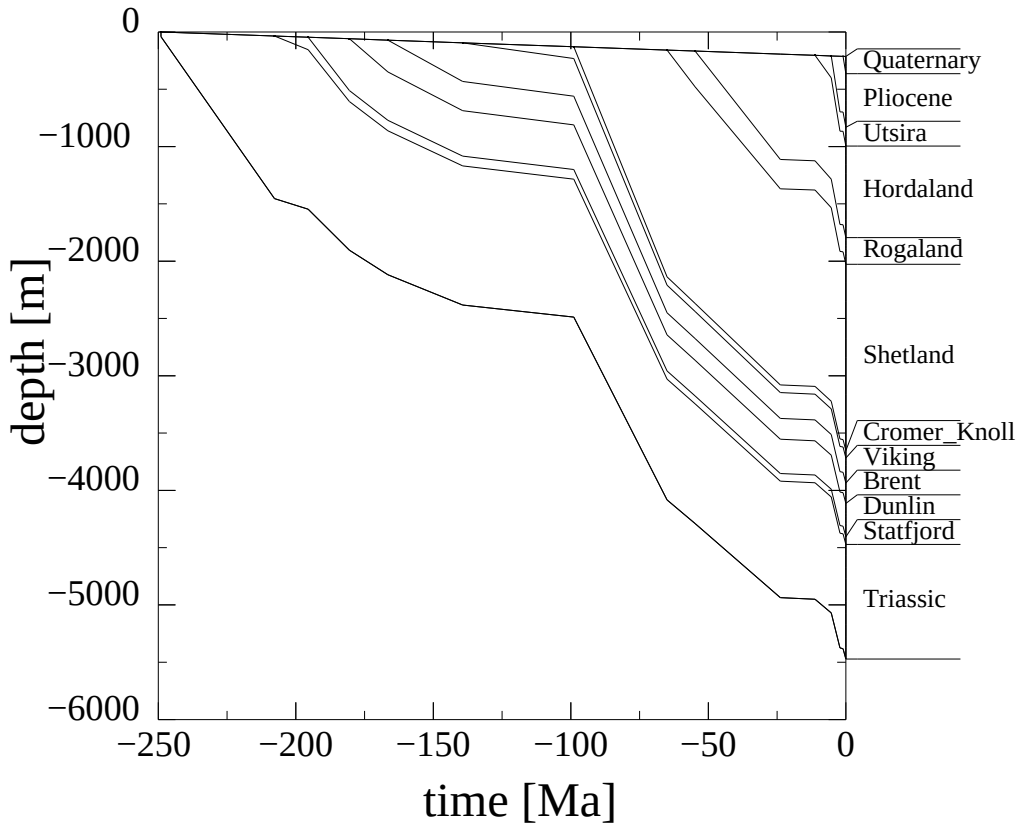
0
−1000
−2000
−3000
−4000
−5000
−6000
depth [m]
−250
−200
−150
−100
−50
0
time [Ma]
Quaternary
Pliocene
Utsira
Hordaland
Rogaland
Shetland
Cromer_Knoll
Viking
Brent
Dunlin
Statfjord
Triassic

fig5.eps

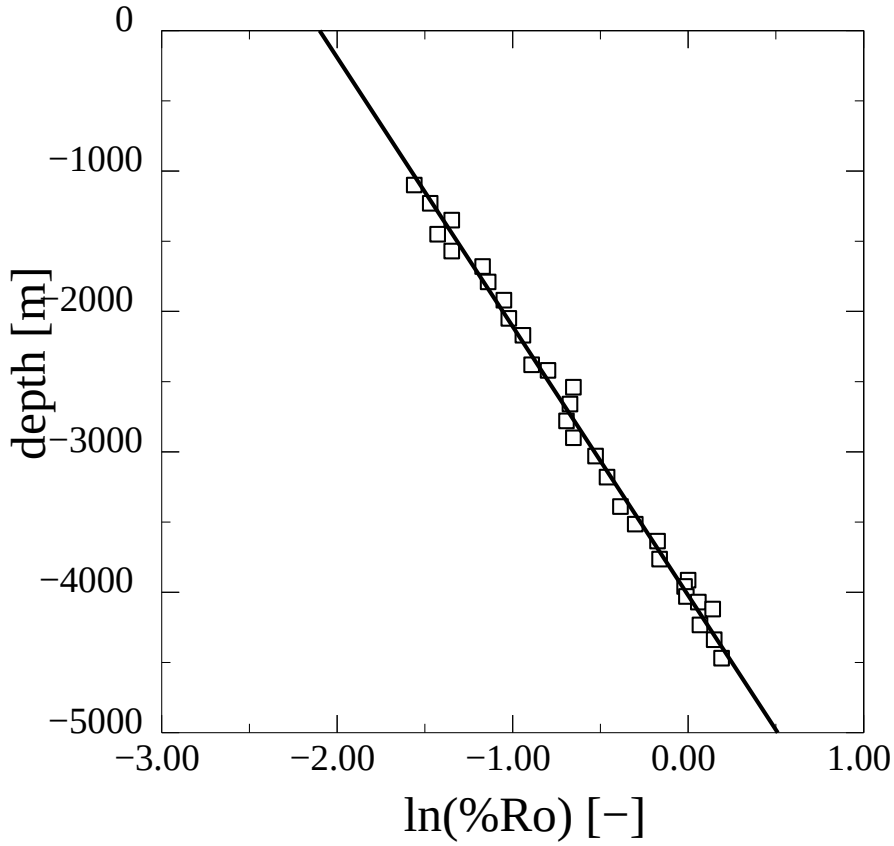

fig6a.eps

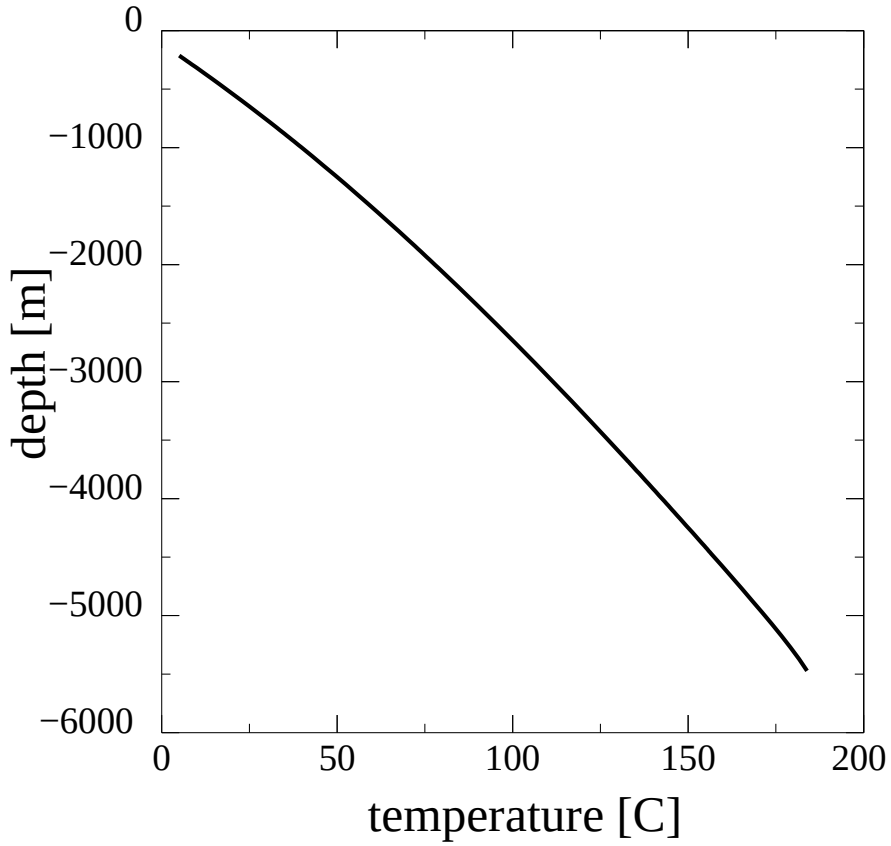
0
−1000
−2000
−3000
−4000
−5000
−6000
depth [m]
0
50
100
150
200
temperature [C]

fig6b.eps

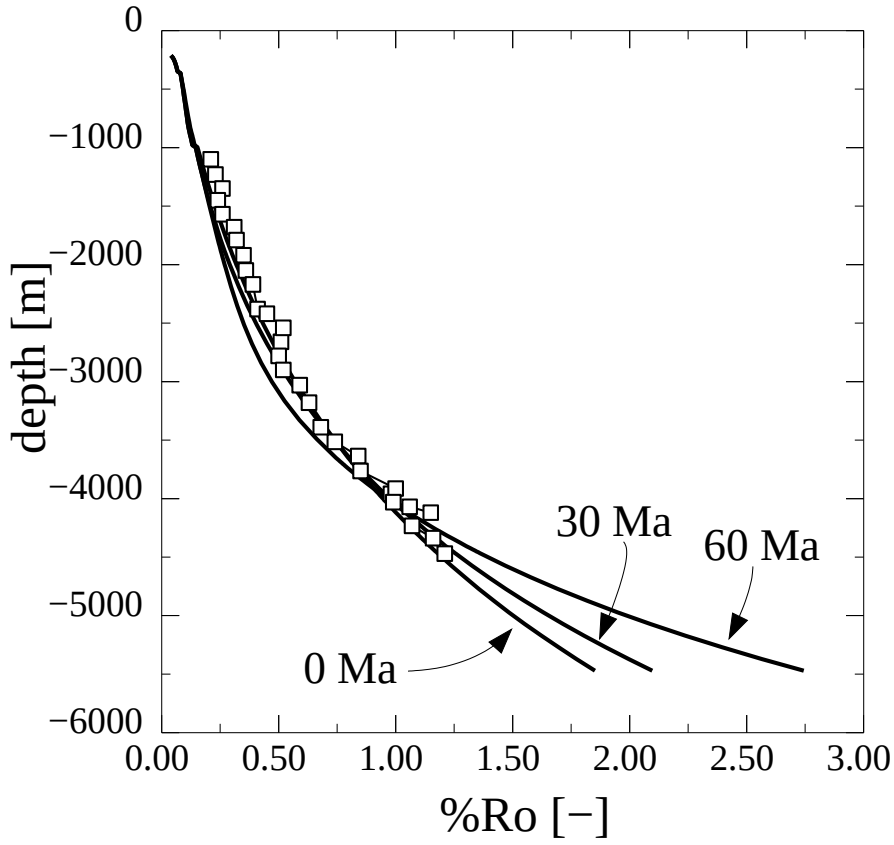
0
−1000
−2000
−3000
−4000
−5000
−6000
depth [m]
0.00
0.50
1.00
1.50
2.00
2.50
3.00
%Ro [−]
30 Ma
60 Ma
0 Ma

fig7a.eps

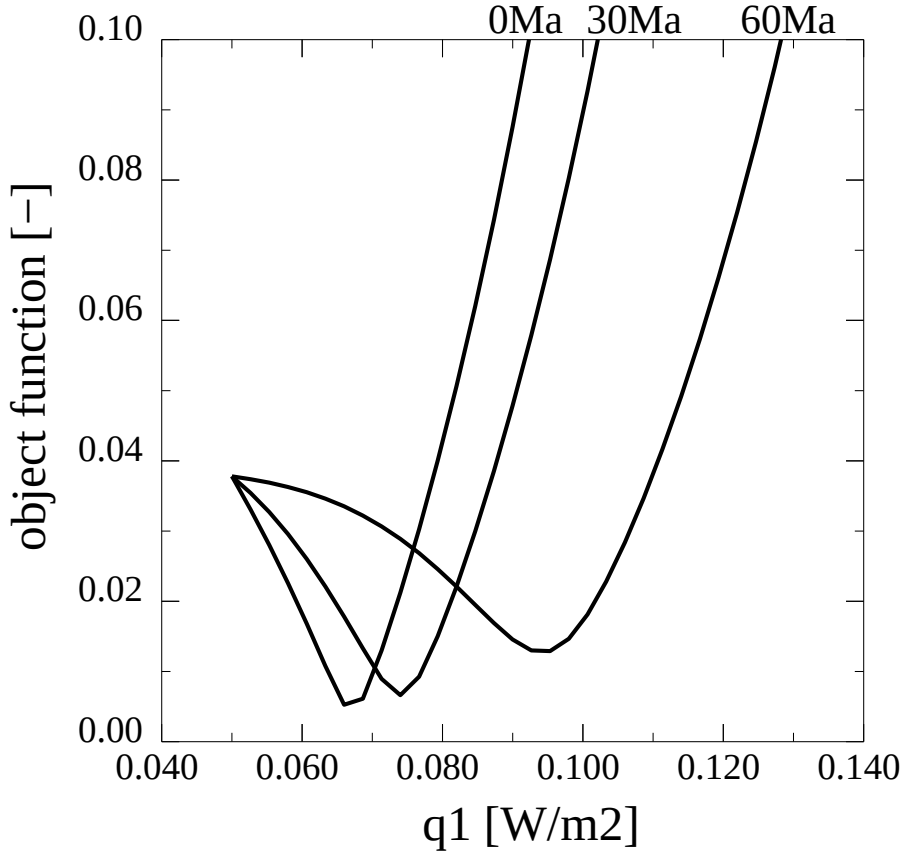
0Ma
30Ma
60Ma
0.10
0.08
0.06
0.04
0.02
0.00
object function [–]
0.040
0.060
0.080
0.100
0.120
0.140
q1 [W/m2]

fig7b.eps

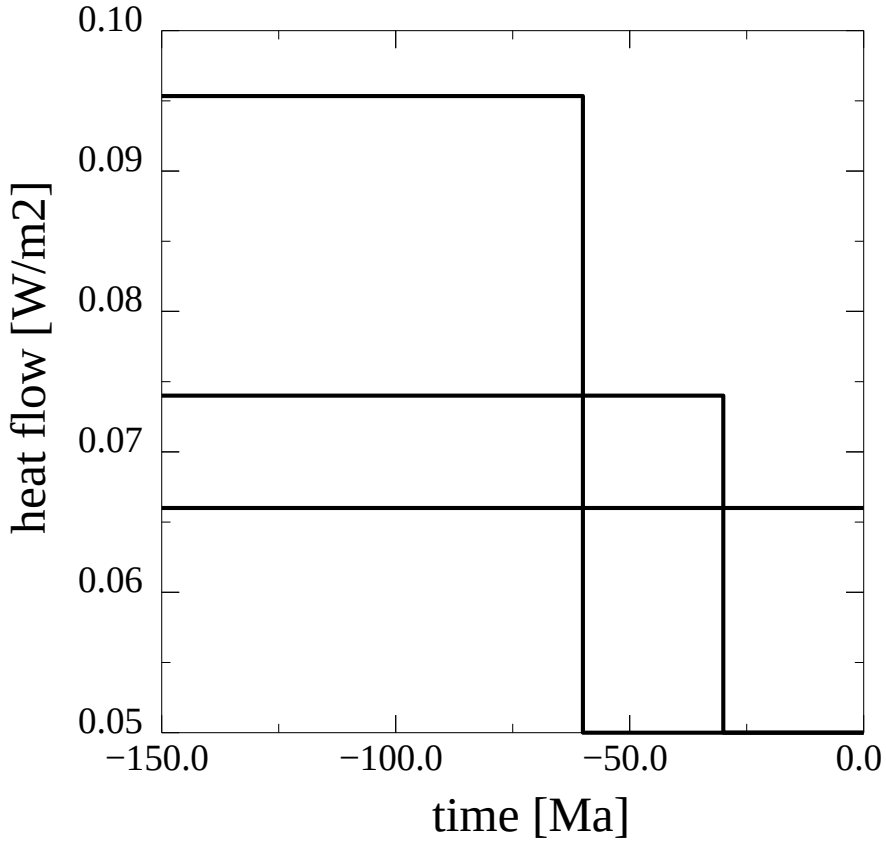

fig7c.eps

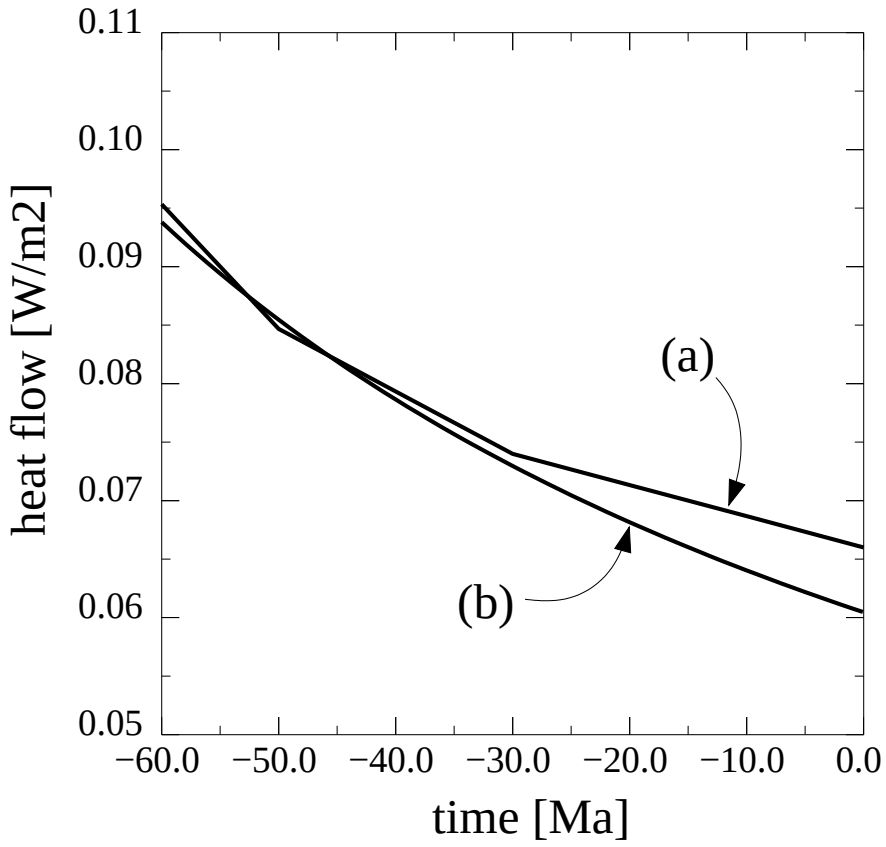
0.11
0.10
0.09
0.08
0.07
0.06
0.05
heat flow [W/m2]
−60.0
−50.0
−40.0
−30.0
−20.0
−10.0
0.0
time [Ma]
(a)
(b)

fig7d.eps

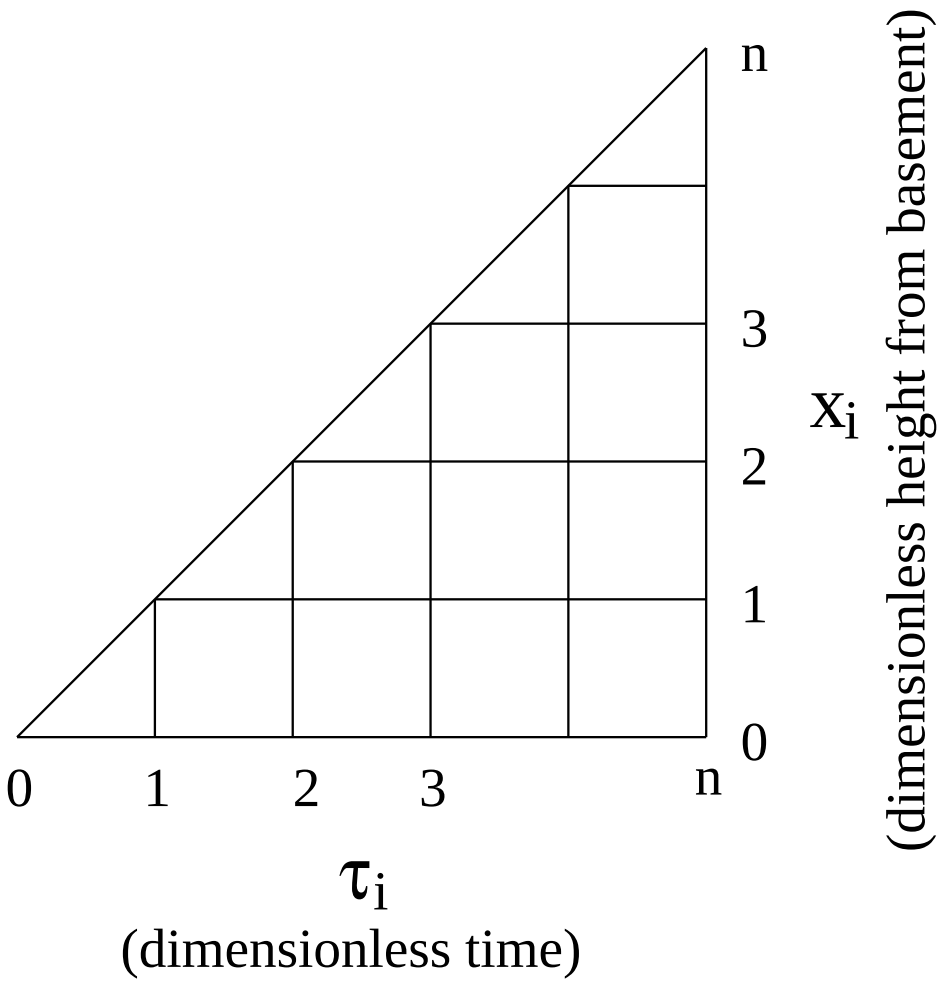
n
3
2
1
0
x_i
(dimensionless height from basement)
0
1
2
3
n
τ_i
(dimensionless time)

fig8.eps

CAPTIONS

Table 1: The parameters are explained in the text, see the given equation.

Figure 1: The paleo heat flow as a step function.

Figure 2a: The modeled VR for four different heat flow histories that all match a VR observation at the base of the well ($x = 0$). The heat flow histories are step functions with a step at $\tau_1 = 0.4$, 0.6, 0.8 and 1. The observed VR at the base of the well is a factor 1.1 higher than the VR obtained from using the reference heat flow for the entire geohistory.

Figure 2b: The same as plot 2a where the VR values are plotted as $\ln(\%Ro)$.

Figure 2c: The optimal paleo heat flow histories that give the modeled VR shown in figure 2a and 2b. The dashed lines show the heat flow histories given by the approximation (15). The approximation is poor for $\tau_1 < 1/2$.

Figure 3a: The modeled VR for four different heat flow histories that all match a VR observation at the base of the well ($x = 0$). The heat flow histories are step functions with a step at $\tau_1 = 0.4$, 0.6, 0.8 and 1. The observed VR at the base of the well is a factor 1.5 higher than the VR obtained from using the reference heat flow for the entire geohistory.

Figure 3b: The same as plot 3a where the VR values are plotted as $\ln(\%Ro)$.

Figure 3c: The optimal paleo heat flow histories that gives the modeled VR shown in figure 3a and 3b. The dashed lines show the heat flow histories given by the approximation (15). The approximation is poor for $\tau_1 < 1/2$.

Figure 4a: The modeled VR for two different histories that both match a VR observation at the base of the well ($x = 0$). The heat flow histories are step functions with a step at $\tau_1 = 0.92$ and 1. The observed VR at the base of the well is a factor 0.9 less than the VR obtained from using the reference heat flow for the entire geohistory.

Figure 4b: The same as plot 4a where the VR values are plotted as $\ln(\%Ro)$.

Figure 4c: The optimal paleo heat flow histories that give the modeled VR shown in figure 4a and 4b. Notice that it is sufficient to apply the reference day heat flow for just the last part of the burial history to achieve the observed VR at the base of the well. The approximate heat flow histories match almost exactly the optimal heat flow histories.

Figure 5: The burial history of a well in the North sea.

Figure 6a: The VR-observations (open squares) plotted as $\ln(\%Ro)$ of depth are following a linear trend.

Figure 6b: The present day geotherm is slightly curved because the average thermal conductivity increases with decreasing porosity.

Figure 7a: The VR observations (open squares) plotted against the modeled VR for three different heat flow histories. The heat flow histories have a step at 0 Ma, 30 Ma and 60 Ma before present.

Figure 7b: The root-mean-square deviation between the VR observations and the modeled VR as a function of the step size in the heat flow history.

Figure 7c: Three heat flow histories that have a step at 0 Ma, 30 Ma and 60 Ma before present.

Figure 7d: Curve (a) is the optimal step size q_1 as a function of the time of the step. Curve (b) is an approximate step size obtained by using equation (15).

Figure 8: The burial history is divided into n parts, where the heat flow is constant in each part.